Consensus Control of Distributed Robots Using Direction of Arrival of Wireless Signals

Ramviyas Parasuraman[1,2] and Byung-Cheol Min[1]

[1] SMART Lab, Department of Computer and Information Technology, Purdue University, West Lafayette, IN 47907, USA
[2] Department of Computer Science, University of Georgia, Athens, GA 30602, USA
email: ramviyas@uga.edu, minb@purdue.edu

Abstract. In multi-robot applications, consensus control and coordination are vital and potentially repetitive tasks. To circumvent practical limitations such as a global localization system, researchers have focused on bearing-based consensus controllers, but most assumed that measurements from sensors (e.g. vision) are noise-free. In this paper, we propose to use wireless signal measurements to estimate the direction of arrival (relative bearings) of neighboring robots and introduce a weighted bearing consensus controller to achieve coordinate-free distributed multi-robot rendezvous. We prove that the proposed controller guarantees connectivity maintenance and convergence even in the presence of measurement noise. We conduct extensive numerical simulation experiments using the Robotarium multi-robot platform to verify and demonstrate the properties of the proposed controller and to compare the performance of the rendezvous task against several state-of-the-art rendezvous controllers.

Keywords: multi-robot systems, consensus, rendezvous, wireless signals, DOA

1 Introduction

Multi-robot rendezvous [1,2] has significance in applications such as battery recharging, collaborative task handling, and information exchange [3,4]. Although significant work has been done on consensus control, prior studies often make strong assumptions such as the global coordinates of the robots being obtainable through localization sensors (e.g. GPS, LIDAR) [5]. However, it is difficult to satisfy these assumptions, especially when confronted with indoor, underground, or cluttered environments.

Alternatively, bearing-based controllers have been proposed to realize consensus control without coordinates [6,7,8]. Vision-based sensors have been exploited as a sensing modality [9], but they require proper lighting conditions and clear line-of-sight, and are susceptible to distance/bearing range limitations. Therefore, there is a need for novel sensing modalities that avoid such limitations in order to estimate relative bearings. Moreover, the design of a consensus controller should consider robustness to noise as any sensor is susceptible to measurement noise.

Wireless devices and received signal strength (RSS) measurements have recently garnered interest in mobile robot sensing [10,11]. Notably, the direction of arrival (DOA) of the RSS can be estimated using directional and omnidirectional antennas [12,13,14]
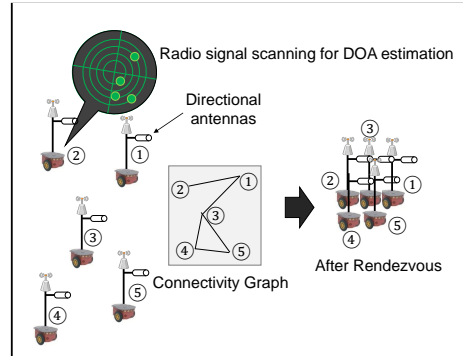
Fig. 1. Illustration of the proposed weighted bearings-based robust coordinate-free distributed consensus controller using the DOA of the wireless signals. The robots are controlled using control inputs calculated based on the relative bearing (DOA) measurements with noise and are weighted by the corresponding RSS values.

and has been exploited in a number of robotic applications such as source tracking, navigation, and teleoperation [15,16,17,18]. However, to date, these measures have not been fully exploited in the aspects of multi-robot consensus control and coordination.

This paper contributes to the field in the following ways:

- First, we propose that the wireless signal RSS and DOA can be used as a sensing modality in distributed multi-robot applications (specifically, for *rendezvous*). The DOA provides the relative bearing between any two robots, assuming that all robots are equipped with a wireless access point (AP) acting as a signal source and a wireless adapter acting as a signal sensor. Figure 1 illustrates the proposed concept.
- Second, taking inspirations from [19,20], we introduce a rendezvous control law (termed *weighted bearings*) that uses the RSS and DOA measurements to achieve distributed coordinate-free consensus control. We theoretically prove that the proposed consensus controller converges (to a rendezvous point) even in presence of measurement noise and maintains connectivity (links) with its neighbors.
- Third, we demonstrate the practical performance of the proposed control scheme through extensive simulation experiments using the Robotarium [21] platform [1].
- Fourth, we compare the proposed controller with state-of-the-art (SOTA) consensus controllers [6,7], using the linear coordinate-based controller [5] as baseline, and analyze the performance in terms of convergence, scalability (increasing size of robots), robustness to sensor noise (errors in bearing measurements), and the control behavior when static (time-invariant) or dynamic network topology is used.

Lastly, we provide open-source software code (in GitHub[2]) for implementations of the proposed controller and SOTA methods in the Robotarium testbed to mutually benefit the community and to develop this research further.

---

[1]Robotarium is a freely accessible remote multi-robot software and hardware testbed provided by Georgia Tech, available at https://www.robotarium.gatech.edu.

[2]Available at https://github.com/SMARTlab-Purdue/robotarium-rendezvous-RSSDOA.

2 Related Work

The rendezvous control problem of multi-robot systems has been extensively studied [22,23,24,25]. Thanks to significant developments in wireless technology in recent decades, wireless networks have been used for connectivity and interaction topology in distributed robotic systems [19]. In most studies, robot states (e.g. relative position in a global coordinate frame) are shared between the robots in order to reach a consensus position (e.g. using geometric features such as the circumcenter). Relatively few studies have addressed the rendezvous problem without sharing coordinates [8,26]. In such cases, local sensors such as vision can be used to detect and identify neighboring robots and to direct the rendezvous process in a distributed fashion [9].

In [6], bearings-only control laws were proposed that used either all relative bearings or only the span angles of the circular sector encompassing all neighbor robots. In [7], the proposed control law assumed pseudo-positions for the neighbor robots based on their relative bearings and the sensing range. Then, the robots moved towards the center of the smallest circle that encompassed all neighbor robot pseudo-positions. In addition, coordinate-free formation (shape) controllers that do not need an external positioning or coordinate referencing system have been well-studied [27,28].

Inspired by the above-mentioned works, we present a novel distributed bearing-aided rendezvous control using DOA and RSS measurements from wireless devices onboard the mobile robots as an alternative sensing modality for bearing estimation. Previous studies demonstrated that DOA can be estimated with reasonable accuracy using minimal hardware and software modification to mobile robots [12,15,29], which highlight the merits of the proposed control scheme.

Finally, even though the sensor data that control robot dynamics are not noise-free in practice, only a handful of studies such as [30,31,32] have considered noisy sensor measurements. Instead, researchers focused on incorporating robustness to failure in the robots or in their connectivity (e.g. using stochastic optimal controllers) [23,2]. Therefore, we experimentally analyze the impact of measurement errors and the effect of time-varying network topology on the performance of the rendezvous controllers compared in this paper.

3 Background

In this section, we present some brief background information relevant to this paper.

Radio Signal Strength (RSS) When a radio signal propagates from a source (e.g. Wi-Fi router) to a destination (e.g. Wi-Fi adapters), its strength attenuates depending on the environmental factors such as the distance (path loss), objects in the environment (shadowing) and spatio-temporal dynamics (multipath fading). A frequently used model to represent the RSS as a function of distance d and time t is given by [33]:

$$R_{(d,t)} = R_{d_0} - 10\eta \log_{10}(\frac{d}{d_0}) - \Psi_{(d)} - \Omega_{(d,t)}(\text{dBm}), \qquad (1)$$

where $R_{d_0} = P_T + G_t + G_r - 20\log_{10}(\frac{4\pi f_c}{c})$ is the RSS at a reference distance d_0 (typically 1m), which depends on the transmit power (P_T), antenna gains (G_t, G_r), and

the radio frequency used (f_c). η is the path loss exponent of a given environment. $d = ||x - x_s||$ is the distance of the receiver (at position x) from the radio source (at position x_s). $\Psi \sim \mathcal{N}(0, \lambda)$ is a Gaussian random variable typically used to represent shadowing, while Ω is a Nakagami-distributed variable representing multipath fading. The model in Eq. (1) has shown in [34,16,35,36] to accurately represent the measurements.

Graph Theory Let $\mathcal{G} = (\mathcal{V}, \mathcal{E})$ denotes an undirected weighted graph with set of vertices (robot nodes) $\mathcal{V} \in \mathbb{R}^N$, edges set $\mathcal{E} = \{(i, j) \subset \mathcal{V} \times \mathcal{V} \,|\, i \in \mathbb{N}_j\}$. The adjacency matrix is $\mathcal{A} = [a_{ij}]_{N \times N}$. For each robot i, its set of neighbors is denoted as $\mathbb{N}_i = \{j \in \mathcal{V} | (i, j) \in \mathcal{E}\}$, and the cardinality of the set $\mathbb{N}_i$ (number of neighbors) is $|\mathbb{N}_i| \in \mathbb{R}^N$. The weights $a_{ij} = 1$, if $(i,j) \in \mathcal{E}$ (if there is a connection between i and j). otherwise, $a_{ij} = 0$. We assume the following properties of the graph: $\mathcal{G}$ is symmetric (i.e. $a_{ij} = a_{ji}$); there is no self-loop and repetitions of edges (i.e. $a_{ii} = 0$); and $\mathcal{G}$ is bidirectional (i.e. $i \in \mathbb{N}_j \leftrightarrow j \in \mathbb{N}_i$).

Problem statement Consider a set of N non-holonomic mobile robots in a workspace $\mathcal{W} \subset \mathbb{R}^d$ (we assume $d = 2$ in this paper[3]) with their state denoted as (position) $q_i = [x_i, y_i]^T \in \mathbb{R}^2$ and (orientation) $\theta_i, i \in \mathcal{V} = [1, 2, ..., N]$, defined in the inertial (world) frame $\mathcal{F}_{\mathcal{W}}$. Their unicycle kinematics is governed by

$$\begin{cases} \dot{x}_i & = u_i \cos\theta_i \\ \dot{y}_i & = u_i \sin\theta_i \\ \dot{\theta}_i & = \omega_i, \end{cases} \tag{2}$$

where $u_i \in \mathbb{R}$ is the linear velocity input, and $\omega_i \in \mathbb{R}$ is the angular velocity input. Let us suppose that the robot i has a local coordinate frame $\mathcal{F}_i$ that is attached to $\mathcal{F}_W$ and the rotation matrix that maps the local coordinate frame to the global frame is given by $\mathcal{R}(\theta_i) = \begin{bmatrix} \cos\theta_i & \sin\theta_i \\ -\sin\theta_i & \cos\theta_i \end{bmatrix}$. Note, we use the superscript i on a variable to explicitly indicate that the variable is expressed in the local frame $\mathcal{F}_i$, otherwise the variable is expressed in the world frame.

Definitions and Assumptions We will use the following definitions and assumptions.

Assumption 1 *A robot senses and communicates with another robot when their relative distance is within the sensing range, i.e. $\|q_j - q_i\| \leq S_{max} \implies j \in \mathbb{N}_i$.*

Definition 1. *The graph $\mathcal{G}$ is connected if there is a communication path from every robot to every other robot in $\mathcal{V}$ as per Definition 1.*

Assumption 2 (Merge) *Two robots merge into one if the distance between them is within a small threshold $\epsilon \in \mathbb{R}_+$.*

Definition 2 (Consensus). *The robots achieve rendezvous if all their positions merge to a common point over time, i.e. when $\lim_{t \to \infty}(q_i - q_j) = 0$, $\forall i, j \in \mathcal{V}$.*

---

[3]Note the problem can be adapted to higher dimensions (e.g. for aerial and underwater vehicles).

Definition 3 (Coordinate-free). *A control law is coordinate-free if each robot can work independently with its local coordinate frame of reference [37].*

Assumption 3 *The connectivity (interaction) graph $\mathcal{G}$ is initially connected as per Definition 1, but not necessarily fully (completely) connected, i.e. $\mathbb{N}_i \geq 1 \,\forall i \in \mathcal{V}$.*

Problem 1. Assume that the robot i uses a bearing sensor to measure the relative bearings ϕ_j^i of its neighbors $j \in \mathbb{N}_i$ with a measurement noise. The measured relative bearing is

$$\tilde{\phi}_j^i = \phi_j^i + \gamma_j, \tag{3}$$

where γ_j is a random variable representing measurement noise. For theoretical analysis, we assume in this paper that $\gamma_j = \mathcal{N}(0, \sigma^2)$ is Gaussian-distributed, which is a standard assumption to represent bearing measurement errors in numerical simulations [30,38,29]. Recall that the superscript i denotes the corresponding variable/measurement in the local frame $\mathcal{F}_i$.

The goal is to design a distributed coordinate-free control law to drive all the N robots to a common location and achieve rendezvous. That is, for a controller $[u_i^i, \omega_i^i]^T = f(\tilde{\phi}_j^i) \,\forall j \in \mathbb{N}_i$, derive a function of relative bearings $f(.)$, which guarantees convergence, maintains connectivity, and is robust to noise in bearing measurements.

4 Proposed Consensus Control Approach

We briefly discuss several approaches to estimate the DOA of the RSS and then introduce the proposed controller.

4.1 Estimation of DOA from the RSS

For brevity, we do not focus on the estimation of the DOA itself in this paper, but we list below three potential approaches that can be used to estimate DOA from RSS measurements depending on the hardware configuration of the robots.

1. Apply vector additions on the measurements from directional antenna arrays [15].

$$\tilde{\phi}_j^i = \arctan\Big(\frac{R_j^{FR} + R_j^{FL} - R_j^{BR} - R_j^{BL}}{R_j^{FR} + R_j^{BR} - R_j^{FL} - R_j^{BL}}\Big), \forall j \in \mathbb{N}_i, \tag{4}$$

   where R_j^{XX} is the RSS (from AP on robot j) measured using a squared planar directional antenna arrangement (FR - Front Right, FL - Front Left, BR - Back Right, BL - Back Left) mounted on robot i. The measured bearing is already aligned on the robot's frame $\mathcal{F}_i$ due to the geometric placement of antennas. Here, the measurement of ϕ_j^i is instantaneous (no delay between measurements).
2. Apply Weighted Centroid Algorithm (WCA) on the RSS measured from a rotating directional antenna [12,17].

$$\tilde{\phi}_j^i = \frac{\sum_{k=1}^{m} b(k)\theta_i^i(k)}{\sum_{k=1}^{m} b(k)}, \; b(k) = 10^{\frac{R_j(k)}{\Gamma}}, \forall j \in \mathbb{N}_i, \tag{5}$$

where $R_j(k)$ is the RSS measured (of wireless signals coming from AP of robot j) using a rotating directional antenna mounted on robot i with an orientation θ_i^i. The robot makes a 360 degree scan (in m different instants) and simultaneously measures $R_j(k)$ from all robots in scanning range. Γ represents a positive gain value. Here, a full rotational scan is needed to estimate the ϕ_j^i (there is a delay between successive measurements at different robot positions due to the rotation).

3. Calculate RSS gradients using measurements from spatially distributed RSS measurements from an omnidirectional antenna [13,14,29,39].

$$\tilde{\phi}_j^i = \arctan \frac{\beta_y}{\beta_x}, \forall j \in \mathbb{N}_i, \tag{6}$$

where $\beta = (X^T X)^{-1} X^T R_j^i$ is the calculated RSS gradients, and $R_j \in \mathbb{R}^{nx1}$ being the vector of n number of RSS (of AP on robot j) measured at non-colinear positions of robot i (in $\mathcal{F}_i$), which are denoted by the vector $X \in \mathbb{R}^{n \times 2}$. Here, a specific movement by the robot is needed to gather adequate non-colinear measurements.

For estimating DOA from RSS measurements in our numerical analysis, we envisage the first approach (planar directional antenna array [15]) because it provides highly accurate instantaneous DOA estimate without restricting the robot's mobility. Nevertheless, as mentioned in Sec. 3, the RSS and DOA measurements are prone to noise and fading effects, therefore the consensus controller should be robust to sensor noise.

4.2   Weighted Bearing Rendezvous Controller

We use the wireless network topology to build the interaction graph $\mathcal{G}$. We propose the following non-linear controller to address the problem described in Sec. 3.

Controller 1 (Weighted Bearing Controller)

$$\begin{bmatrix} u_i \\ \omega_i \end{bmatrix} = \frac{v_{max}}{|\mathbb{N}_i|} \sum_{j \in \mathbb{N}_i} w_{ij} \begin{bmatrix} \cos \tilde{\phi}_j^i \\ \sin \tilde{\phi}_j^i \end{bmatrix},$$

$$w_{ij} = \frac{1}{-(R_{th} - R_j^i)}, \tag{7}$$

where R_{th} is the threshold RSS power[4], R_j^i is the RSS measured at robot i coming from the AP of robot j, and ϕ_j^i is the DOA measured by robot i from j in the local frame $\mathcal{F}_i$ (Sec. 4.1) because the controller is expressed in the local frame $\mathcal{F}_i$. The controller can be applied in the global frame $\mathcal{F}_W$ (single-integrator dynamics) using the rotational transformation as

$$\begin{bmatrix} \cos \tilde{\phi}_{ij}^W \\ \sin \tilde{\phi}_{ij}^W \end{bmatrix} = \mathcal{R}(\theta_i) \begin{bmatrix} \cos \tilde{\phi}_j^i \\ \sin \tilde{\phi}_j^i \end{bmatrix} \text{ and } \dot{q}_i = \begin{bmatrix} \dot{x}_i \\ \dot{y}_i \end{bmatrix} = u_i^W \begin{bmatrix} \cos \theta_i \\ \sin \theta_i \end{bmatrix}. \tag{8}$$

---

[4]We assume RSS is measured in dBm as provided by most Wi-Fi manufacturers. However, to retain the exponential mapping of the signal power with distance, we convert the RSS in dBm to Watts using $R(W) = E^{-3} 10^{\left[\frac{R(dBm)}{10}\right]}$ for use in our controller.

Note, since the RSS is a naturally decreasing function of the inter-robot distance $\|q_{ij}(t)\|$, as per the Eq. (1), the weights w_{ij} are state-dependent. However, the weights are normalized to bound the command inputs and to minimize the impact of geometric bias and sensor noise among the RSS measurements of the neighbor robots.

Theorem 1 (Convergence and Stability). *Under the control law in Eq.* (7) *with the noisy RSS measurements, the group of robots converges to a single point within a small threshold over time (Definition 2) and achieves rendezvous if Assumption 3 holds true.*

Proof. We first prove the nonlinear system stability without noise. And then, we incorporate noise in our analysis through a discretized dynamical system.

Consider that the measured bearing is noise-free, ϕ_j^i. To prove the convergence, we follow Lyapunov control approach similar to [6,26]. We need to prove that for each robot i, the sum of relative distances between all its neighbors $\sum_{j \in \mathbb{N}_i} \|q_j - q_i\| \Rightarrow 0 \, \forall i \in \mathcal{V}$ as $t \to +\infty$. Using this as a Lyapunov candidate function, the total displacement Energy value is given by,

$$V = \sum_{i \in \mathcal{V}} \sum_{j \in \mathbb{N}_i} \|q_{ij}\| = \sum_{i \in \mathcal{V}} \sum_{j \in \mathcal{V}} a_{ij} \|q_j - q_i\|. \tag{9}$$

Here, the adjacency index $a_{ij} = 1$ if robots i and j are neighbors, and $a_{ij} = 0$ otherwise. Using Eq. (2), we have the time derivative of V as

$$\dot{V} = \sum_{i \in \mathcal{V}} \sum_{j \in \mathcal{V}} a_{ij} \frac{(q_j - q_i)^T}{\|q_j - q_i\|} (\dot{q}_j - \dot{q}_i). \tag{10}$$

As we assume an undirected graph, $a_{ij} = a_{ji}$ and $\dot{q}_j = -\dot{q}_i$. Therefore,

$$\dot{V} = -2 \sum_{i} \sum_{j \in \mathcal{V}} a_{ij} \frac{(q_j - q_i)^T}{\|q_j - q_i\|} \dot{q}_i, \tag{11}$$

After some manipulations with the help of Eq. (8) and (2), we obtain

$$\dot{V} = -2 \sum_{i \in \mathcal{V}} \sum_{j \in \mathcal{V}} a_{ij} u_i \cos \phi_{ij}^w \tag{12}$$

$$\dot{V} = -2 \sum_{i \in \mathcal{V}} u_i \sum_{j \in \mathcal{V}} a_{ij} \cos \phi_{ij}^w \leq 0. \tag{13}$$

Thus, we show that the Lyapunov function is negative semidefinite. The derivative $\dot{V}$ is 0 only when the velocity $u_i = 0$ for all robots $i \in \mathcal{V}$. The largest invariance set (with assumption 2) is $\dot{V} = 0$ when $u_i = 0$, which can occur even when $\|q_{ij}\| \neq 0$ (not all robots converged at equilibrium point with $V = 0$). However, when $u_i = 0$ and $\|q_{ij}\| \neq 0$, then $\omega_i \neq 0$ because the projection matrix of ω_i is orthogonal to that of u_i (Eq. (8) and (7)) (i.e., $\begin{bmatrix} u_i \\ \omega_i \end{bmatrix} \neq \begin{bmatrix} 0 \\ 0 \end{bmatrix}$). This will eventually drive at least one robot in the system to a different state where $u_i \neq 0$, thus making $\dot{V} < 0$. Also, the weights asymptotically decay with the distance. Therefore, according to LaSalle

invariance principle [40], the system asymptotically converges to a common state and achieve rendezvous. This concludes the first part of the proof.

Now assume a noisy measurements as in Eq. (3) for DOA (e.g., [29,38]). Following the approach in [31], we use the condition that the expected value of stochastic control input caused by the measurement noise has the same sign as that of the noise-free (deterministic) control input. i.e. $\mathbb{E}[\tilde{u}_i] \cdot u_i \geq 0$. Through the Lyapunov analysis of the discrete dynamical system, we have

$$\dot{V} = -2\sum_{i \in \mathcal{V}} |\mathbb{N}_i| (\sum_{j \in \mathcal{V}} a_{ij} \mathbb{E}[w_{ij}] \mathbb{E}[\cos \phi_{ij}^w])(\sum_{j \in \mathcal{V}} a_{ij} \mathbb{E}[\cos \phi_{ij}^w]) \leq 0. \tag{14}$$

Although both w_{ij} and bearing ϕ_j^i depend on the RSS measurements, they are independent of each other because of the different time instants when the measurements are made. For instance, for the bearing estimation, the RSS measured in all the sensors or rotation angles are used, whereas for weights only one instant of the measurements are used. This potentially results in $\mathbb{E}[\tilde{u}_i] \cdot u_i \geq 0$. Therefore, the noise will not affect the system stability. This concludes the proof.

Theorem 2. *Connectivity maintenance: Under the control law in Eq.* (7) *with the Assumptions in Sec. 3, the graph $\mathcal{G}$ remains connected throughout the rendezvous process.*

Proof. To prove this, we use the same approach as the Preposition 5.1 of [19]. The weights w_{ij} in Eq. (7) act as the artificial potential field to the controller. The R_{th} is defined by the sensing range S_{max} (in our case, the sensitivity of the wireless receiver). Both R_{th} and R_j^i in w_{ij} depend on the distance between the robots and therefore, are indirect representation of distance measurements. This enables us equate our controller weights to the distance-based weights analyzed in [19]. We have that,

$$\lim_{\|q_{ij}\| \to S_{max}} w_{ij} = \infty. \tag{15}$$

Although we do not explicitly state the proof here, we can show that the derivative of the potential field after introducing a hysteresis into the system is non positive (i.e. $\dot{w}_{ij} \leq 0$), similar to [19]. Thus, all the links in $\mathcal{G}$ are maintained, which ensures that the graph is always connected at all instants during the rendezvous process.

5   Numerical Validation

To prove the concept of the proposed rendezvous controller, we conducted simulation experiments using the *Robotarium* framework [21]. We chose the Robotarium because it provides testbeds for both simulations and real experiments with the GRITSbot robots using the same software codes. Although Robotarium provides a barrier certificate utility function to avoid collisions between robots, this function may affect the outcome and the performance of the algorithm execution, and thus we did not use them in our experiment to obtain a fair comparison.

To simulate the RSS measurements, we used Eq. (1) with the following parameters that are typically used in wireless network simulations: RSS_{d_0} = -20 dBm; η = 3; and

$\lambda = 4$ dBm [34]. Due to the small size of the Robotarium environment (3m x 3m), we applied a scaling factor of 50 to achieve a larger simulation area (150m x 150m) and obtain realistic Wi-Fi RSS simulations. We simulated the DOA by measuring relative bearing through the Robotarium state information and added a zero-mean Gaussian noise (as observed in [29,38,30]). The sensing range is set to $S_{max} = 0.8m$ ($40m$ in the scaled-up environment).

5.1   Scenarios

We consider the following three scenarios:

Scenario 1 - Multiple Trials with Randomized Initial Positions We verify the proposed controller with SOTA methods by conducting 10 trials for each controller with random initial positions of the robots. For each controller, the Robotarium iterates max 1000 times. In addition, to analyze the effect of the size of the multi-robot system, we perform experiments with an incremental number of the robots in the system $N = (5, 10, 20)$.

Scenario 2 - Impact of Bearing Measurement Errors We analyze the impact of measurement noise by simulating noisy sensor data in the bearing measurement system. For a fair comparison of all the bearings-based controllers, in this experiment, we added a standard normal distribution to simulate the γ in Eq. (3) with a variance $0 \leq \sigma \leq 1.35$ radians, under two experiments with a different number of robots $N = (8, 15)$.

Scenario 3 - Impact of Network Topology Updates We compare the performance of the controllers using a fixed network (interaction) topology and a dynamic network topology under two sensor noise conditions. Note that for Scenarios 1 and 2, the interaction topology is dynamically updated by default. This scenario is used mainly to analyze how the controllers perform in static interaction topology.

5.2   Comparison with SOTA Methods

We compare the proposed rendezvous controller (**Controller 1**) with the following baseline and the SOTA methods.

Baseline - Coordinates-based [5] This method is one of the most used consensus controlled methods available in the literature that uses coordinates of all the robots. We used this method as a baseline (**Controller 2**) and hypothesize that our proposed strategy achieves performance similar to this baseline method.

Bearings-only controllers We implemented three SOTA bearing based controllers. Two of them are from [6], where we use bearings of all the neighbors (**Controller 3**) and only the min and max bearings of the neighbors (**Controller 4**). The other bearing based controller (**Controller 5**) is the implementation of enclosing circles [7].

	Controller 1 RSS and DOA (Proposed)	Controller 2 Using Coordinates (Baseline) [5]	Controller 3 All Bearings SOTA [6]	Controller 4 Min and Max Bearings SOTA [6]	Controller 5 Enclosing Circles SOTA [7]	Controller 6 Weighted Bearing (Proposed)
First three values: Distance traveled traveled by all robots (Max, Mean and SD) averaged over several trials (m). Last two values: Maintained Connectivity? (Y/N), Iteration # at the Stop Condition.						
Scenario 1 : Verifying Convergence and Scalability ($\sigma = 0$)						
N = 5	**1.44**, **1.60**, 0.10, Y, **211**	1.32, 1.43, 0.19, Y, 476	1.98, 1.82, 0.11, Y, 233	1.87, 1.79, 0.10, Y, 226	2.02, 1.84, 0.12, Y, 229	1.87, 1.78, 0.11, Y, 222
N = 10	2.45, 2.21, 0.15, Y, 353	1.84, 1.72, 0.08, N, 333	2.38, 2.22, 0.11, N, 340	2.28, 2.06, 0.18, N, 569	2.29, 2.13, 0.15, Y, 517	**1.99**, **1.84**, 0.13, N, **338**
N = 15	4.15, 3.89, 0.14, Y, 373	3.06, 2.86, 0.10, Y, 387	4.14, 3.94, 0.11, N, 340	3.71, 3.38, 0.22, N, 642	9.22, 8.98, 0.15, Y, **338**	**3.16**, **2.86**, 0.20, N, 372
N = 20	4.99, 4.73, 0.15, Y, 359	3.66, 3.51, 0.08, Y, 344	4.86, 4.68, 0.10, N, 297	4.30, 3.87, 0.24, Y, 635	22.50, 22.02, 0.26, Y, 957	**3.24**, **2.96**, 0.20, Y, 385
Scenario 2 : Verifying Robustness to Sensor Noise						
No Noise ($\sigma = 0$, N=8)	2.35, 2.28, 0.11, Y, **390**	1.78, 2.23, 0.10, Y, 411	2.30, 2.28, 0.11, Y, 496	1.99, 2.26, 0.10, Y, 426	2.19, 2.26, 0.11, Y, 419	**1.90**, **2.24**, 0.11, Y, 408
With Noise ($0.15 \leq \sigma \leq 1.35$, N=8)	2.40, 2.14, 0.16, Y, 503	1.73, 1.63, 0.09, Y, 404	2.34, 2.14, 0.15, Y, 673	2.41, 2.22, 0.14, N, 630	2.44, 2.27, 0.13, Y, 822	**2.03**, **1.92**, 0.06, Y, **501**
No Noise ($\sigma = 0$, N=15)	3.12, 2.37, 0.21, Y, 553	2.30, 2.29, 0.11, Y, 564	3.36, 2.39, 0.19, N, **492**	3.10, 2.33, 0.34, N, 736	5.41, 2.60, 0.25, Y, 533	**2.31**.**2.27**, 0.24, Y, 569
With Noise ($0.15 \leq \sigma \leq 1.35$, N=15)	3.28, 2.89, 0.21, Y, 661	2.34, 2.22, 0.08, N, 552	3.31, 3.03, 0.19, N, **559**	3.26, 2.85, 0.19, N, 945	4.27, 4.05, 0.12, Y, 956	**2.46**, **2.28**, 0.11, Y, 711
Scenario 3 : Verifying Robustness to Topology Updates (N=15)						
Graph Not Updated ($\sigma = 0$)	4.09, 3.71, 0.27, Y, **483**	2.58, 2.25, 0.19, Y, 510	3.92, 3.77, 0.14, N, 1000	3.62, 3.38, 0.16, Y, 911	3.51, 3.11, 0.25, Y, 906	**3.44**, **2.91**, 0.33, Y, 524
Graph Not Updated ($\sigma = 0.5$)	4.13, 3.73, 0.24, Y, **507**	2.48, 2.16, 0.18, Y, 515	4.06, 3.79, 0.16, N, 1000	3.79, 3.59, 0.13, Y, 1000	3.97, 3.72, 0.12, Y, 1000	**3.76**, **3.39**, 0.15, Y, 528
Graph Updated ($\sigma = 0.5$)	4.06, 3.70, 0.21, Y, 570	2.94, 2.79, 0.10, Y, 562	4.28, 3.88, 0.22, N, **481**	4.12, 3.69, 0.29, N, 558	5.27, 5.08, 0.13, Y,1000	**3.06**, **2.86**, 0.12, Y, 590

Table 1. Summary of the results of the evaluation metrics defined in Sec. 5.3 obtained in all the scenarios. The best values other than the Baseline is highlighted in Bold.

Range-weighted bearings controller Further, we also implemented a distance-weighted bearing controller based on distance and DOA measurements (**Controller 6**), which is a minor variant of connectivity-preserving rendezvous control in [19]. This controller also holds the same properties as our *Weighted Bearings* controller but require both distance and bearing sensors. For more information on all the SOTA controllers compared in this paper, please see the supplementary video available in YouTube[5].

5.3   Evaluation metrics

We used the following metrics to evaluate the performance of the consensus controller:

- **Energy**: the Lyapunov candidate function in Eq. (9).
- **Distance**: the max, mean and standard deviation of the total distance traveled by all the robots averaged over time (iterations).
- **Speed of convergence**: the number of iterations taken to achieve the stop condition which is to reach all the neighbor robots within 0.1m by all the robots.
- **Time performance**: the time taken to achieve the rendezvous conscience process.
- **Connectivity preservation**: whether the final graph is connected or not (Yes/No) in all the trails of a particular condition.

6   Results

In Table 1, we summarize the results of the experiments for all the evaluation metrics. Below, we present the convergence results of individual scenarios.

6.1   Scenario 1

Figure 2 shows the energy function value over the iteration averaged over 10 trials each for experiments with up to 20 number of robots. In table 1, we present the evaluation metrics distance traveled and time performance. In Figure 2 (left), it shows that the

---

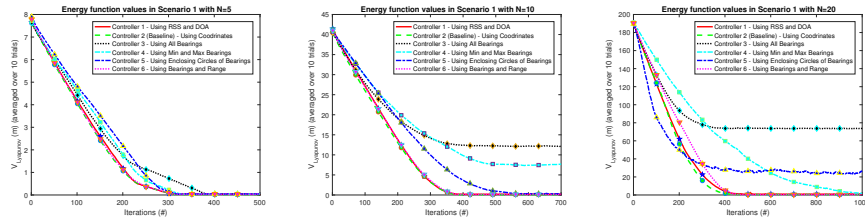[5] Details on the SOTA controllers and the results are shown in https://youtu.be/6BkFrJ8vceg.

Fig. 2. Convergence of the energy function averaged over 10 trials (each with random initial positions) in Scenario 1 with increasing number of robots.
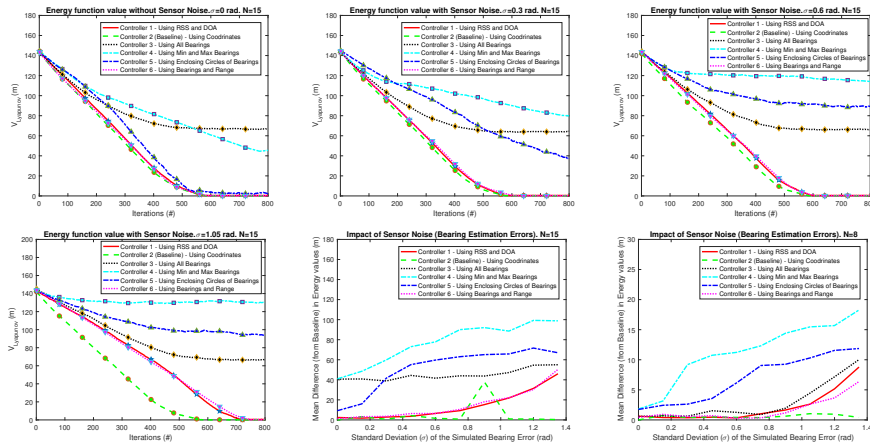

Fig. 3. Convergence of the energy function in Scenario 2 with increasing noise (errors) in bearing sensor measurements.

proposed controller, Controller 1, converged at the almost same time as the baseline and Controller 6, while Controller 2. Controller 3, Controller 4, and Controller 5 were also able to converge, but it is noticed that their convergences were slower than Controller 1. This figure clearly validates that the proposed controller guarantee convergence and excel the SOTA controllers in terms of convergence when $N = 5$.

In Figure 2 (center), we increased the number of robots, i.e. $N = 10$. In this scenario, again our Controller 1 converged at the almost same time as the baseline like the scenario when $N = 5$. Controller 5 that uses enclosing circles was also able to converge although the time of its convergence was slower than the proposed controller and the baseline. However, Controller 3 and Controller 4 failed to converge in this scenario because some robots were disjointed from the other group.

In Figure 2 (right), we further increased the number of robots, i.e. $N = 20$. As a result, our proposed controller, Controller 1 using RSS and DOA, performs the best convergence, followed by the baseline. Controller 6 also shows that it performs well although its convergence rate was slightly slower than those of Controller 1 and the Controller 2. Interestingly, the convergence rate of the Controller 5 was faster than all
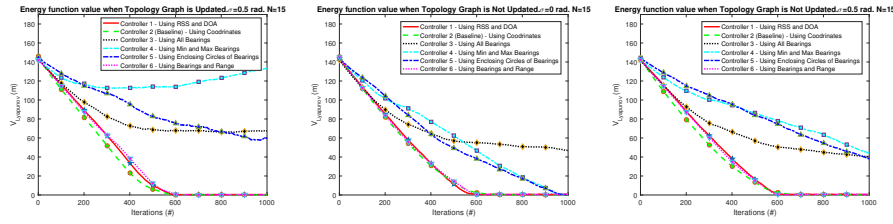
Fig. 4. Convergence of the energy function in Scenario 3 with and without the update of network topology graph in every iteration (only the initial graph is considered if not updated) under two sensor noise conditions. Note: the top left plot in Fig. 3 (update of topology, but no sensor noise) should be used as a reference to these plots.
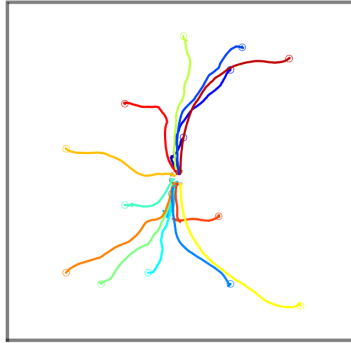

Fig. 5. An sample screenshot of one of the simulation experiments in the Robotarium, where $N = 15$ and $\sigma = 0.35$ rad. The initial positions of the robots are indicated by circles.

the others during 0 to 200 iterations, but it could not converge in the end. Similarly, Controller 3 using all bearings also fails to converge in this scenario, while Controller 4 was able to converge with the slowest convergence rate among the successful controllers.

From this result, we can validate that the proposed controller guarantee convergence as well as scalability.

6.2   Scenario 2

In Fig. 3, we show the effect of an arbitrary sensor noise resulted from bearing sensor measurements on the consensus control performance using the energy function values. In this scenario, we used 15 mobile robots ($N = 15$) with the same initial positions for all controllers. The top three figures and the bottom left figure show convergence of all the 6 controllers without and with sensor noise (varying from $\sigma = 0.3$ to $\sigma = 1.05$). When there was no sensor noise (top right figure), the performances of the controllers were similar to those with Scenario 1 with $N = 10$, where the proposed Controller 1 and Controller 6, converged well and outperformed the other controllers. Controller 3 and Controller 4 failed to converge due to some of the disjointed robots. And, even
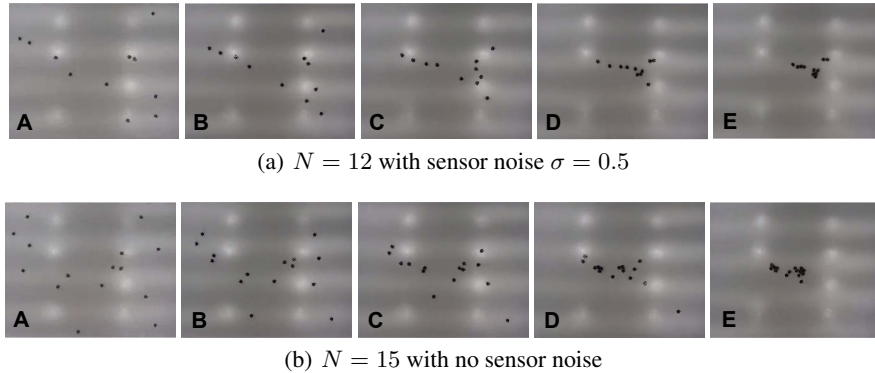
(a) $N = 12$ with sensor noise $\sigma = 0.5$

(b) $N = 15$ with no sensor noise

Fig. 6. Sample experiments with real robots in the Robotarium testbed. The temporal sequence is sorted alphabetically.

when there was sensor noise, the proposed controller show that they converge although their convergence rates were slower than the baseline, particularly when $\sigma = 1.05$. On the other hand, the SOTA methods (Controllers 3-5) failed to converge.

The bottom right two figures show the mean differences from the baseline to the five controllers with respect to the different sensor noise values with $N = 15$ (left) and $N = 8$ (right). As shown in these figures, when the sensor noise values $\sigma \leq 0.5$, the Controller 1 and Controller 6, performed well and showed the similar performance of the baseline, although their performance is gradually degraded as the sensor noise value is increased. On the other hand, the SOTA controllers showed large mean differences for all different sensor noise values. From this scenario, we could validate that the proposed controller is robust to errors in sensor measurements.

6.3 Scenario 3

In Fig. 4, we compare the outcomes of the rendezvous with and without a network topology update under the following conditions: $N = 15$ and without and with sensor noise ($\sigma = 0.5$). As a result, it is shown that the Controller 1 and Controller 6 are robust to both cases when a network topology graph is updated and not updated with sensor noise. On the other hand, the other SOTA controllers failed to converge for the most cases. Particularly, when there was sensor noise, the SOTA controllers failed to converge regardless of whether the a time-variant or time-invariant topology is used. From this scenario, we could validate that the proposed controller perform well no matter static or dynamic network topology, unlike the other SOTA controllers.

6.4 Discussions

For our experimental analysis, we ran simulations (see an example in Fig. 5) in the Robotarium as it gave us a leverage of using more than 15 robots, which is the current limit for hardware (on real robots) experiments in Robotarium. Nevertheless, we replicated a

few of simulation experiments on real robots (see an example in Fig. 6, where the robots converge around the consensus point within a small threshold distance from each other) and found that the robots are able to achieve consensus using the simulated DOA measurements, closely matching with the results obtained in simulation analysis. However, further investigation is required to validate the proposed method in practice using real DOA measurements on real robots, which also justify the assumptions and models used in this research. For that, we will explicitly use one of the DOA methods mentioned in Sec. 4.1 and plan to conduct extensive hardware experiments on real robot platforms in the near future to validate the proposed controller, including addressing the implementation aspects of the DOA and RSS measurements from multiple neighbor robots.

In summary, we conducted extensive experiments using the Robotarium platform to validate the proposed weighted-DOA based consensus controller (sample simulation and real experiments are presented in Fig. 5 and Fig. 6, respectively) and compared its performance in rendezvous tasks with those of state-of-the-art rendezvous control laws. In the experiments, we demonstrated that the proposed controller excels the SOTA in terms of convergence and scalability ($5 < N < 20$), robustness to bearing measurements (up to a Gaussian noise of $\mathcal{N}(0, 1.2^2)$), and is indifferent to static/dynamic interaction topologies, while the SOTA is not robust to those conditions/errors. We used Lyapunov method to guarantee the stability of the non-linear system through the assumption of an undirected graph. Similarly, the sensing approach we used (wireless medium) enabled us to assume a symmetric graph. In future, we will analyze the proposed controller on the directed graph and non-symmetric graphs.

7   Conclusions

In this paper, we proposed a new distributed *Weighted Bearing* consensus control law for multi-robot rendezvous. Our key approach is using wireless signal measurements as a sensing modality to estimate DOA (relative bearings weighted by the RSS) of neighboring robots and use in distributed multi-robot rendezvous. From the extensive experiments, we demonstrate that the proposed approach does not require an external positioning system, guarantees convergence and stability, maintains connectivity with neighboring robots, and is robust to sensor measurement errors.

In future works, we plan to conduct field experiments with networked mobile robots equipped with all necessary equipment for the proposed system. To do so, we will implement the proposed controller and integrate it with the obstacle avoidance algorithm during the rendezvous benefiting from our prior works (e.g. DOA from RSS and DOA from SONARs). We will also examine the performance of the proposed rendezvous control law under harsh conditions such as faults in robots and network disruptions.

References

1. Lin, J., Morse, A., Anderson, B.: The multi-agent rendezvous problem. an extended summary. In: Cooperative Control, pp. 257–289. Springer (2005)
2. Dimarogonas, D.V., Kyriakopoulos, K.J.: On the rendezvous problem for multiple nonholonomic agents. IEEE Transactions on Automatic Control **52**(5), 916–922 (2007). DOI 10.1109/TAC.2007.895897

3. Li, B., Moridian, B., Mahmoudian, N.: Underwater multi-robot persistent area coverage mission planning. In: OCEANS 2016 MTS/IEEE Monterey, pp. 1–6 (2016). DOI 10.1109/OCEANS.2016.7761238

4. Mathew, N., Smith, S.L., Waslander, S.L.: A graph-based approach to multi-robot rendezvous for recharging in persistent tasks. In: Robotics and Automation (ICRA), 2013 IEEE International Conference on, pp. 3497–3502. IEEE (2013)

5. Jadbabaie, A., Lin, J., Morse, A.S.: Coordination of groups of mobile autonomous agents using nearest neighbor rules. In: Proceedings of the 41st IEEE Conference on Decision and Control, 2002., vol. 3, pp. 2953–2958 vol.3 (2002). DOI 10.1109/CDC.2002.1184304

6. Zheng, R., Sun, D.: Rendezvous of unicycles: A bearings-only and perimeter shortening approach. Systems & Control Letters **62**(5), 401–407 (2013)

7. Kriegleder, M., Digumarti, S.T., Oung, R., D'Andrea, R.: Rendezvous with bearing-only information and limited sensing range. In: Robotics and Automation (ICRA), 2015 IEEE International Conference on, pp. 5941–5947. IEEE (2015)

8. Yu, J., LaValle, S.M., Liberzon, D.: Rendezvous without coordinates. IEEE Transactions on Automatic Control **57**(2), 421–434 (2012). DOI 10.1109/TAC.2011.2158172

9. Lopez-Nicolas, G., Aranda, M., Mezouar, Y., Sagues, C.: Visual control for multirobot organized rendezvous. IEEE Transactions on Systems, Man, and Cybernetics, Part B (Cybernetics) **42**(4), 1155–1168 (2012)

10. Banfi, J., Li, A.Q., Basilico, N., Rekleitis, I., Amigoni, F.: Multirobot online construction of communication maps. In: 2017 IEEE International Conference on Robotics and Automation (ICRA), pp. 2577–2583 (2017). DOI 10.1109/ICRA.2017.7989300

11. Ghaffarkhah, A., Mostofi, Y.: Communication-aware motion planning in mobile networks. IEEE Transactions on Automatic Control **56**(10), 2478–2485 (2011)

12. Min, B.C., Matson, E.T., Jung, J.W.: Active antenna tracking system with directional antennas for enhancing wireless communication capabilities of a networked robotic system. Journal of Field Robotics **33**(3), 391–406 (2016)

13. Twigg, J.N., Fink, J.R., Yu, P., Sadler, B.M.: RSS gradient-assisted frontier exploration and radio source localization. In: IEEE International Conference on Robotics and Automation (ICRA), pp. 889–895. IEEE (2012)

14. Parasuraman, R., Fabry, T., Molinari, L., Kershaw, K., Castro, M.D., Masi, A., Ferre, M.: A Multi-Sensor RSS Spatial Sensing-Based Robust Stochastic Optimization Algorithm for Enhanced Wireless Tethering. Sensors **14**(12), 23,970–24,003 (2014). DOI 10.3390/s141223970

15. Caccamo, S., Parasuraman, R., Båberg, F., Ögren, P.: Extending a ugv teleoperation flc interface with wireless network connectivity information. In: 2015 IEEE/RSJ International Conference on Intelligent Robots and Systems (IROS), pp. 4305–4312. IEEE (2015)

16. Gil, S., Kumar, S., Katabi, D., Rus, D.: Adaptive communication in multi-robot systems using directionality of signal strength. The International Journal of Robotics Research **34**(7), 946–968 (2015)

17. Min, B.C., Parasuraman, R., Lee, S., Jung, J.W., Matson, E.T.: A directional antenna based leader–follower relay system for end-to-end robot communications. Robotics and Autonomous Systems **101**, 57–73 (2018)

18. Owen-Hill, A., Parasuraman, R., Ferre, M.: Haptic teleoperation of mobile robots for augmentation of operator perception in environments with low-wireless signal. In: 2013 IEEE International Symposium on Safety, Security, and Rescue Robotics (SSRR), pp. 1–7. IEEE (2013)

19. Zavlanos, M., Egerstedt, M., Pappas, G.: Graph theoretic connectivity control of mobile robot networks. Proceedings of IEEE **99**(9), 1525–1540 (2011)

20. Zheng, R., Sun, D.: Multirobot rendezvous with bearing-only or range-only measurements. Robotics and Biomimetics **1**(1), 4 (2014). DOI 10.1186/s40638-014-0004-5

21. Pickem, D., Glotfelter, P., Wang, L., Mote, M., Ames, A., Feron, E., Egerstedt, M.: The robotarium: A remotely accessible swarm robotics research testbed. In: Robotics and Automation (ICRA), 2017 IEEE International Conference on, pp. 1699–1706. IEEE (2017)
22. Ji, M., Egerstedt, M.: Distributed coordination control of multi-agent systems while preserving connectedness. IEEE Transactions on Robotics **23**(4), 693–703 (2007)
23. Park, H., Hutchinson, S.: An efficient algorithm for fault-tolerant rendezvous of multi-robot systems with controllable sensing range. In: Robotics and Automation (ICRA), 2016 IEEE International Conference on, pp. 358–365. IEEE (2016)
24. Setter, T., Egerstedt, M.: Energy-constrained coordination of multi-robot teams. IEEE Transactions on Control Systems Technology (2016)
25. Feng, Z., Sun, C., Hu, G.: Robust connectivity preserving rendezvous of multi-robot systems under unknown dynamics and disturbances. IEEE Transactions on Control of Network Systems **PP**(99), 1–1 (2016). DOI 10.1109/TCNS.2016.2545869
26. Zhao, S., Zheng, R.: Flexible bearing-only rendezvous control of mobile robots. In: 2017 36th Chinese Control Conference (CCC), pp. 8051–8056. IEEE (2017)
27. Montijano, E., Cristofalo, E., Zhou, D., Schwager, M., Sagüés, C.: Vision-based distributed formation control without an external positioning system. IEEE Transactions on Robotics **32**(2), 339–351 (2016)
28. Das, A.K., Fierro, R., Kumar, V., Ostrowski, J.P., Spletzer, J., Taylor, C.J.: A vision-based formation control framework. IEEE Transactions on Robotics and Automation **18**(5), 813–825 (2002)
29. Dantu, K., Goyal, P., Sukhatme, G.S.: Relative bearing estimation from commodity radios. In: IEEE International Conference on Robotics and Automation, 2009. ICRA'09, pp. 3871–3877. IEEE (2009)
30. Tang, Z.J., Huang, T.Z., Shao, J.L.: Consensus of multiagent systems with sampled information and noisy measurements. Discrete Dynamics in Nature and Society **2013** (2013)
31. Gowal, S., Martinoli, A.: Bayesian rendezvous for distributed robotic systems. In: 2011 IEEE/RSJ International Conference on Intelligent Robots and Systems (IROS), pp. 2765–2771. IEEE (2011)
32. Wang, Y., Xie, Y., Cheng, L.: Leader-following consensus of multi-agent systems with dynamic leader and measurement noises. In: 2017 36th Chinese Control Conference (CCC), pp. 8379–8384. IEEE (2017)
33. Rappaport, T.: Wireless Communications: Principles and Practice, 2nd edn. Prentice Hall PTR, Upper Saddle River, NJ, USA (2001)
34. Lindhé, M., Johansson, K.H., Bicchi, A.: An experimental study of exploiting multipath fading for robot communications. In: 3rd International Conference on Robotics Science and Systems, RSS 2007, 27-30 June 2007, Atlanta, GA, USA, pp. 289–296 (2008)
35. Muralidharan, A., Mostofi, Y.: Statistics of the distance traveled until connectivity for unmanned vehicles. arXiv preprint arXiv:1808.02538 (2018)
36. Mostofi, Y., Malmirchegini, M., Ghaffarkhah, A.: Estimation of communication signal strength in robotic networks. In: 2010 IEEE International Conference on Robotics and Automation (ICRA), pp. 1946–1951. IEEE (2010)
37. Aranda, M., López-Nicolás, G., Sagüés, C.: Coordinate-free control of multirobot formations. In: Control of Multiple Robots Using Vision Sensors, pp. 131–181. Springer (2017)
38. Venkateswaran, S., Isaacs, J.T., Fregene, K., Ratmansky, R., Sadler, B.M., Hespanha, J.P., Madhow, U.: Rf source-seeking by a micro aerial vehicle using rotation-based angle of arrival estimates. In: American Control Conference (ACC), 2013, pp. 2581–2587. IEEE (2013)
39. Lowrance, C.J., Lauf, A.P.: Direction of arrival estimation for robots using radio signal strength and mobility. In: Positioning, Navigation and Communications (WPNC), 2016 13th Workshop on, pp. 1–6. IEEE (2016)
40. La Salle, J.P.: The stability of dynamical systems. SIAM (1976)